Chemical characterization of aerosols over the Atlantic Ocean and the Pacific Ocean during two cruises in 2007 and 2008

M. Zhang,[1,2,3] J. M. Chen,[1] T. Wang,[2] T. T. Cheng,[1] L. Lin,[1,3] R. S. Bhatia,[3,4] and M. Hanvey[3,5]

Received 22 March 2010; revised 10 July 2010; accepted 10 August 2010; published 20 November 2010.

[1] To help understand the chemical properties of marine aerosols and the long-distance transport of continental aerosols to remote oceanic regions, total suspended particulates (TSP) samples were collected over the Atlantic Ocean and the Pacific Ocean during two cruises in September–December 2007 (cruise I) and March–April 2008 (cruise II) aboard the M/V *Oceanic II*. Data were analyzed and interpreted with the aid of back trajectory, principal component, and multiple linear regression analyses. Compared with the results over the South Pacific from 2 decades ago, the non-sea-salt sulfate (NSS-SO_4^{2-}) concentrations over the South Pacific have increased by a factor of ~1.5, while the NO_3^- concentration has remained constant. On average, NSS-SO_4^{2-} accounted for 30–52% of the total SO_4^{2-} during the two cruises. Chloride deficit was observed in all samples, with NSS-SO_4^{2-} being the preferred species for acid displacement over the South Pacific and the Mediterranean Sea. Persistent clean marine air masses were only observed over the northern Atlantic and South Pacific during cruise I, while more frequent impacts of continental air (dust, biomass burning, and industrial plumes) were observed during cruise II. Combined with the NAAPS aerosol maps, these results indicate that during cruise II, (1) southern Atlantic was influenced by Southern Africa and the interhemisphere transport of biomass burning plumes in Central Africa, (2) northern Atlantic was under the combined pollution plumes of Sahara dust intrusion and biomass burning, and (3) the Mediterranean Sea was affected by the mixed pollution from biomass burning and industrial contamination, as well as Saharan dust.

Citation: Zhang, M., J. M. Chen, T. Wang, T. T. Cheng, L. Lin, R. S. Bhatia, and M. Hanvey (2010), Chemical characterization of aerosols over the Atlantic Ocean and the Pacific Ocean during two cruises in 2007 and 2008, *J. Geophys. Res.*, *115*, D22302, doi:10.1029/2010JD014246.

1. Introduction

[2] The long-range transport of atmospheric aerosol from continents to the oceans has important implications for ocean ecosystems, climate and atmospheric chemistry. Nutrients from continental aerosols fertilize the ocean water by stimulating phytoplankton growth and thus influence marine geochemical cycle [*Zhuang et al.*, 1992; *Jickells et al.*, 2005]. The continental-derived aerosols also affect radiative balance of the atmosphere over the remote oceans directly by scattering and absorbing solar radiation and indirectly by modifying cloud properties [*Kaufman et al.*, 2002; *Andreae*, 2007; *Intergovernmental Panel on Climate Change*, 2007]. In addition, aerosols can play important roles in tropospheric chemistry via various heterogeneous pathways [e.g., *Laskin et al.*, 2003; *Chen et al.*, 2007].

[3] The physical, chemical and optical properties of aerosols over the Atlantic Ocean have been studied in aircraft campaigns (e.g., TARFOX [*Russell et al.*, 1999] and ACE-2 [*Raes et al.*, 2000]) and cruises [e.g., *Davison et al.*, 1996; *Bates et al.*, 2001; *Lerk et al.*, 2002], as well as using satellite data [*Chiapello and Moulin*, 2002] and long-term ground-based programs [e.g., *Chiapello et al.*, 2005]. These studies have demonstrated the influence of Saharan dust and biomass burning in Africa over the Atlantic Ocean [e.g., *Johansen et al.*, 2000; *Virkkula et al.*, 2006], and the transport of anthropogenic pollution from Africa to North America, and from North America to Europe [e.g., *Riemer et al.*, 2006; *Lelieveld et al.*, 2001; *Han et al.*, 2006]. Most of the previous cruise measurements were conducted near Europe [e.g., *Hoornaert et al.*, 1996; *Ebert et al.*, 2002] and the Canary Islands [e.g., *Hoornaert et al.*, 2003; *Li et al.*, 2003], measurements over the southern parts of the Atlantic Ocean were scarce.

[1]Center for Atmospheric Chemistry, Department of Environmental Science and Engineering, Fudan University, Shanghai, China.
[2]Department of Civil and Structural Engineering, Hong Kong Polytechnic University, Kowloon, Hong Kong.
[3]Formerly at Scholar Ship Research Institute, London, UK.
[4]National Oceanography Centre, Southampton, UK.
[5]Nature Publishing Group, London, UK.

0148-0227/10/2010JD014246

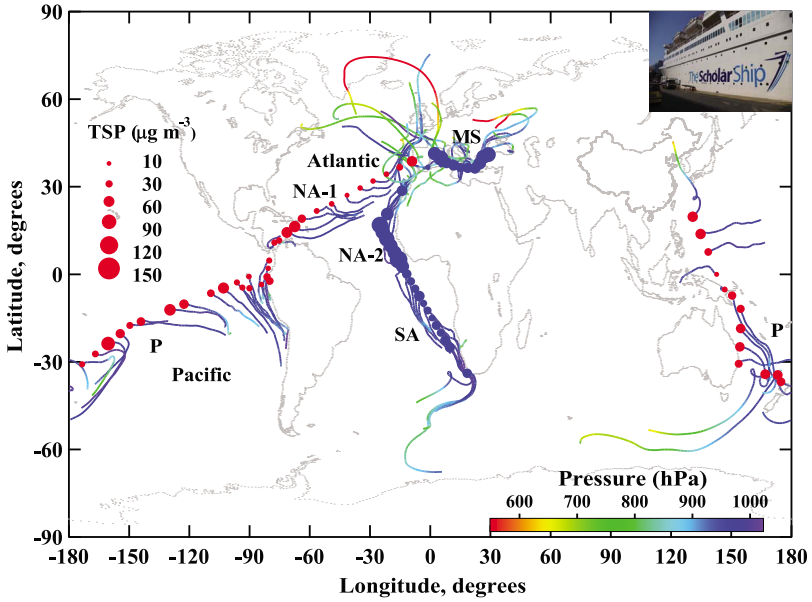

Figure 1. Cruise tracks was dotted by TSP concentrations (red for cruise I and blue for cruise II), with the 5 day air mass back trajectories arriving at 200 m above sea level indicated by color-coded lines.

[4] Over the Pacific Ocean, there has been of considerable interest in the transport of mineral aerosols from the Asian continent [e.g., *Sakai et al.*, 2000; *Talbot et al.*, 1997; *Duce et al.*, 1980]. Several large programs, e.g., SEAREX [*Prospero and Savoie*, 1989; *Gagosian et al.*, 1982], PEM-West A [*Arimoto et al.*, 1996], TRACE-P [*Jacob et al.*, 2003] and ACE-Asia [*Huebert et al.*, 2003], together with several cruises [e.g., *Kaneyasu and Murayama*, 2000; *Tsunogai and Kondo*, 1982; *Covert et al.*, 1996], flights [e.g., *Yamato and Tanaka*, 1994], satellite data [e.g., *Kaufman et al.*, 2002] and long-term islands observation [*Savoie and Prospero*, 1989], over the Pacific Ocean have studied the chemical and physical properties of marine aerosols. Most of these studies were conducted during the 1980s–1990s and early 2000s.

[5] Among various sampling platforms, ship-borne measurements offer some unique aspects. First, while numerous data on atmospheric aerosols are available over lands, there is much less information from open oceans. Second, precise description of aerosol composition over oceans requires in situ ship-based chemical measurements. Finally, ship-based measurements offer necessary data for studying global aerosol transport mechanisms and for validating model simulations and satellite retrievals [*Kaufman et al.*, 2002; *Smirnov et al.*, 2006].

[6] This paper presents the results of an aerosol sampling study during two cruises over the Atlantic Ocean, the Pacific Ocean, and the Mediterranean Sea in 2007 and 2008. We first report the overall concentrations of inorganic ions, elemental carbon (EC), and organic carbon (OC) in five regions, compare the results with those from previous studies. We then examine the contribution of continental aerosols to the marine environment and the chemical interactions between marine and continental aerosols. Of specific interest is to examine the chloride deficit by NO_3^- and NSS-SO_4^{2-} over different oceanic regions. Finally, we assess source attribution in five regions using a principal component analysis and NAAPS aerosol maps.

2. Experimental Setup

2.1. Cruise Tracks

[7] Measurements were taken from a cruise vessel known as The Scholar Ship (M/V *Oceanic II*, http://en.wikipedia.org/wiki/The_Scholar_Ship). The first voyage started from Greece, crossed the Atlantic and Pacific Oceans via the Panama Canal, and finished in Hong Kong (cruise dates September to December 2007). The second voyage sailed from Hong Kong to Thailand, India, South Africa, then north through the Atlantic Ocean to Spain, across the Mediterranean Sea to Turkey, Portugal and finishing in Netherlands (cruise dates January to April 2008). Apart from sampling TSP aerosol, complementary atmospheric observations were made for ozone, NO_X, and meteorological parameters.

[8] The work reported here focuses on the TSP samples collected over parts of the voyages, specifically over the Atlantic Ocean, the Pacific Ocean and the Mediterranean Sea. The following two cruise tracks were of particular interest. Cruise I was for the ship sailing from Lisbon, Portugal (38.72°N, 9.12°W, 19 September 2007), across the Atlantic and Pacific oceans to the eastern China Sea (24.56°N, 127.44°E, 4 December 2007). Cruise II was from Cape Town, South Africa (33.90°S, 18.42°E, 4 March 2008) to Lisbon, Portugal (38.72°N, 9.12°W, 15 April 2008). The cruise tracks are shown in Figure 1, which is dotted according to TSP concentrations, with the 5 day air mass back trajectories arriving at a height of 200 m indicated by color-coded lines. Meteorological profiles (air temperature, relative humidity, pressure, horizontal wind speed/direction, visibility and sky cover) were recorded simultaneously every six hours each day. A Ferrybox, sampling seawater from the engine room,

logged the ship's speed, GPS coordinates and other parameters once each minute.

2.2. Aerosol Collection

[9] TSP samples were collected using a high-volume aerosol sampler (Thermo Fisher Scientific Co., Ltd., Model Andersen GPS1–111 PUF Blower Motor Assembly, flow rate 300 m^3 d^{-1}), which was installed above the bridge at the starboard railing at the uppermost deck of the ship to avoid contamination from the ship exhaust (29 m above sea level). Calibration for flow rate was taken before and after the motor's carbon brush replacement, typically once every month. All samples were collected on Whatman Grade QM-A Quartz Fiber Filters (105 mm diameter, Whatman company, UK). In general, samples were collected over a 24 h period, but due to a more polluted air masses encountered during cruise II, the sampling time was shortened to 12 h during cruise II. Prior to sampling, the filters were wrapped in aluminum foil and preheated at 550°C overnight to remove all organic materials, conditioned in a constant desiccator (20 ± 1°C and 40 ± 2% relative humidity (RH)) for 24 h, and then weighed. When one sampling interval was completed, the sample holder and filter were placed in a clean plastic bag and brought back to a clean laboratory area for unloading. Filter samples were folded in two, with the exposed sides face to face, wrapped in aluminum foil and stored at −20°C in a laboratory refrigerator before analysis at the end of each voyage. All procedures were strictly quality controlled to avoid sample contamination.

2.3. Chemical Analysis

2.3.1. Ion Analysis and Gravimetric Determination

[10] Ten inorganic ions (SO_4^{2-}, NO_3^-, NO_2^-, F^-, Cl^-, Na^+, K^+, Ca^{2+}, Mg^{2+}, NH_4^+) and four organic acids (acetate, formate, methanesulfonic acid (MSA) and oxalate) were analyzed by Ion Chromatography (IC, Dionex 3000, USA), which consists of a separation column (Dionex Ionpac AS 11), a self-regenerating suppressed conductivity detector (Dionex Ionpac ED50) and a gradient pump (Dionex Ionpac GP 50). The gradient weak base eluent (0.3–30mM KOH+H_2O) was used for anion detection, which was over 30 min for each sample. While the weak acid eluent was used (20 mM MSA) for cation detection. The recovery of ions was in the range of 80–120%. The relative standard deviation was less than 5% for reproducibility testing. Quality assurance was routinely carried out by using Standard Reference Materials (GBW 08606) produced by National Research Center for Certified Reference Materials, China. Blank values were subtracted from sample determinations. Details are given elsewhere [*Yuan et al.*, 2003]. Special care was used in IC analysis of particulate matter collected on these quartz fiber filters due to high blank levels [*Chow*, 1995; *Nie et al.*, 2010]. Extraction procedures and blanks correlation are given by *Fermo et al.* [2006].

[11] TSP mass was determined by the difference in filter mass (equilibrated to 20 ± 1°C and 40 ± 2% RH) before and after aerosol collection.

2.3.2. Carbon Analysis

[12] OC and EC were analyzed using a Thermo/Optical Carbon Analyzer (Desert Research Institute (DRI) Model 2001, Atmoslytic Inc., Catabasas, California, USA). A 0.5 cm^2 punch from each filter was analyzed for eight carbon fractions following the IMPROVE (Interagency Monitoring of Protected Visual Environments) thermal optical reflectance (TOR) protocol [*Cao et al.*, 2003; *Chow et al.*, 2004]. This procedure produced: four fractions of OC (OC1, OC2, OC3, and OC4 at 120°C, 250°C, 450°C, and 550°C, respectively, in a He atmosphere); OP (pyrolytic carbon fraction determined when reflected or transmitted laser light attains its original intensity after O_2 is added to the analyzer's atmosphere); and three fractions of EC (EC1, EC2, and EC3 at 550°C, 700°C, and 800°C, respectively, in a O_2/He (2%/98%) atmosphere). The detection limit for the carbon analyzer was 0.05 μg carbon cm^{-2} for a typical punch size of 0.5 cm^2.

2.4. Statistical Analysis

[13] A multivariate statistical analysis was performed using SPSS software [*SPSS, Inc.*, 1997]. Principal component analysis was performed with the output of the varimax rotated component matrix identifying correlations between chemical species and extracting their possible sources. A principal component in this study can represent a source, such as crustal material, sea salt, or an anthropogenic source.

2.5. Complementary Tools

[14] Back trajectory calculations were determined using the HYSPLIT_4 (Hybrid Single Particle Lagrangian Integrated Trajectory) modeling system. This public domain model has been described elsewhere (http://www.arl.noaa.gov/ready/hysplit4.html). GDAS meteorological data was used in the calculations set.

[15] Navy Aerosol Analysis and Prediction System (NAAPS) global aerosol model results were obtained from the Marine Meteorology Division of the Naval Research Laboratory, USA (NRL) (http://www.nrlmry.navy.mil/aerosol). This model is a modified form of that developed by *Christensen* [1997]. The NRL version uses global meteorological fields from the Navy Operational Global Atmospheric Prediction System (NOGAPS) analyses and forecasts on a 1 × 1 degree grid at 6 h intervals and 24 vertical levels reaching 100 mbar [*Hogan and Rosmond*, 1991].

3. Results and Discussion

3.1. Overview of the Expedition

[16] Cruise tracks and TSP concentrations (red for cruise I and blue for cruise II) are presented in Figure 1, with 5 day air mass back trajectories arriving at 200 m above sea level indicated by color-coded lines. In order to examine the data recorded at sea in more detail, the two cruises were divided into five regions. Region 1 (the northern Atlantic Ocean (NA-1 for short) of cruise I, −9.12° < longitude < −75.27°) which was influenced by long-range transport from Europe and North Africa. Region 2 was in the Pacific Ocean (P) from Ecuador to Shanghai during cruise I, which was mostly in the Southern Hemisphere (−30° < latitude < 0°). Region 3 (the Southern Atlantic Ocean (SA), −40° < latitude < 0°) during cruise II was influenced by air masses from central and southern Africa and from the southern Atlantic Ocean. Region 4 (the northern Atlantic Ocean (NA-2), 0° < latitude < 30°) during cruise II was mainly influenced by Europe and North Africa. Region 5 (the Mediterranean Sea (MS)) represented typical European influences and long-range transport from North America.

[17] Table 1 lists the average, standard deviation, and the concentration range of TSP mass, ions, OC, and EC in the five regions excluding samples collected in ports and those contaminated by ship's own emissions. Sea salt (SS) and non-sea-salt (NSS) contributions to SO_4^{2-}, Cl^-, F^-, K^+, Mg^{2+}, and Ca^{2+} are determined from measured Na^+ concentrations and the constant ratio of these species expected in seawater [*Millero and Sohn*, 1992], assuming that Na^+ is a conservative tracer of sea salt. The mean TSP concentrations in five regions varied from 20.1 ± 9.0 $\mu g\ m^{-3}$ to 81.9 ± 20.3 $\mu g\ m^{-3}$. Region NA-2 was characterized by the highest mean TSP and most of ion species concentrations (except EC and Cl^-), indicating strongest influence of continental air masses. While the lowest mean TSP and ion species concentrations (except NO_3^-, Cl^-, OC and EC) were observed in region NA-1, reflecting clean marine conditions.

[18] The longitudinal and latitudinal variations of the concentrations of TSP, total water-soluble ions, OC and EC during cruise I and cruise II are shown in Figure 2. The maximum TSP of 116.1 $\mu g\ m^{-3}$ was observed in NA-2 on 12 March 2008 (latitude: 5.00° to 7.46°, longitude: −15.72° to −17.75°) and the minimum of 10.4 $\mu g\ m^{-3}$ was observed in NA-1 on 24 September 2007 (latitude: 27.11° to 24.18°, longitude: −41.47° to −49.06°). There was a clear north-south gradient in TSP and total water-soluble ions concentrations during cruise II. The mass ratio of total ions plus EC and OC to TSP was 0.30–0.85 during cruise I and 0.17–0.93 during cruise II. As expected, the NaCl from sea salt has a large portion. More discussions on the contributions from various sources will be given in section 3.4.

3.2. Comparison With Previously Published Data

[19] The TSP concentrations in the northern part of the South China Sea in this study were similar to those obtained from other recent studies [*Zhang et al.*, 2007]; however the TSP concentrations near the Cape Verde Islands over the northern Atlantic Ocean were ~1.5 times higher than 60 $\mu g\ m^{-3}$ reported by *Johansen et al.* [2000]. The mean value 20.1 ± 9.0 $\mu g\ m^{-3}$ in NA-1 during cruise I was close to the background level of the eastern North Atlantic subtropical region (~14 $\mu g\ m^{-3}$) [*Alonso-Pérez et al.*, 2007]. Below we compare the chemical composition data with those in other studies.

3.2.1. Major Ions

[20] $SS\text{-}SO_4^{2-}$, $NSS\text{-}SO_4^{2-}$, NO_3^-, and $NO_3^-/NSS\text{-}SO_4^{2-}$ ratios are shown in Figure 3. The $NSS\text{-}SO_4^{2-}$ concentrations we observed over the South Pacific (P, 0.64 ± 0.48 $\mu g\ m^{-3}$) appear to have increased by a factor of ~1.5 higher than those measured on several islands over a similar sampling period over the South Pacific 2 decades ago [*Savoie and Prospero*, 1989]. Our measured NO_3^- concentration over the South Pacific is in close agreement with the 0.11 $\mu g\ m^{-3}$ observed by *Prospero and Savoie* [1989]. We can estimate the impact of continental nitrate over the Northern Hemisphere if we assume that the NO_3^- values measured in the South Pacific are representative of the oceanic "background" and that these values are applicable to the oceans in the Northern Hemisphere. By assuming a "background" level of NO_3^- to be 0.12 ± 0.15 $\mu g\ m^{-3}$, the continental sources appear to have contributed 82% (NA-1), 89% (SA), 92% (NA-2) and 87% (MS) to the total NO_3^- observed. The measurements for $NSS\text{-}SO_4^{2-}$ over NA-2 (1.90 ± 0.48 $\mu g\ m^{-3}$) is a factor of ~1.5 higher than corresponding observations by *Johansen et al.* [2000].

[21] On average, 43% (NA-1), 30% (P), 42% (SA), 52% (NA-2) and 29% (MS) of the total SO_4^{2-} is from non-sea-salt derived. These ratios are in good agreement with those determined in a number of studies carried out over the Northern Atlantic Ocean [*Sievering et al.*, 1991, 1995] showing high wind speed increasing this percentage (Tables 2 and 3). Laden with a large portion of NSS, coarse aerosols experience high rates of dry deposition which results in rapid recycling of ocean-derived sulfur. This process has been overlooked or understated in Remote Marine Boundary Layer (RMBL) sulfur budget analyses and models [*Sievering et al.*, 2004]. Weighted linear regression analysis [*Johansen et al.*, 1999] has been used in this study to extract biogenic SO_4^{2-} contributions. While it could not be consistently extracted probably due to the varying air mass characteristics and temperature throughout the duration of our two cruises (table is not shown here).

[22] The mass ratio $NO_3^-/NSS\text{-}SO_4^{2-}$ has been used by some investigators to identify the origin of air masses [e.g., *Berresheim et al.*, 1991; *Ellis et al.*, 1993; *Li-Jones and Prospero*, 1998]. A mass ratio of 0.4 is typically found in European air masses, while a ratio of ~1.1 have been observed in air masses from the southwest of sub-Saharan Africa. As shown in Figures 3c and 3d, we observed a mass ratio of 0.5–1.0 for NA-1, 0.0–0.5 for P, 1.0–1.5 for SA and 0.5–1.0 for NA-2, while the ratios for MS showed larger ranges. The large variation in $NO_3^-/NSS\text{-}SO_4^{2-}$ makes it difficult to use these ratios for an accurate identification of source regions. Nonetheless, they provide some indicative values for the three regions.

[23] For cations (auxiliary material Figures S1a–S1h), total Na^+ concentrations (Table 1) are within the range previously observed in Barbados, Cape Verde, and the Atlantic [*Johansen et al.*, 2000, and references therein].[1] The NSS contribution of water-soluble K^+ was greater in cruise II than cruise I (auxiliary material Figures S1c and S1d), contributing 69% to the total water-soluble K^+ during cruise II. $NSS\text{-}K^+$ and oxalate are both good tracers for biomass burning [*Saarikoski et al.*, 2007], with the highest value seen in NA-2. During cruise II (5–22 March 2008) hot spots/fires (http://maps.geog.umd.edu/firms/) are presented in central Africa ($-10° <$ latitude $< 15°$), which is consistent with the analysis of source attribution (section 3.4) indicating that samples in cruise II were influenced by biomass burning plumes from central Africa.

[24] On average, NSS Mg^{2+} accounts for 18.5 ± 7.0% (NA-1), 8.3 ± 7.2% (P), 34.6 ± 11.2% (SA), 16.6 ± 8.2% (NA-2) and 13.1 ± 16.6% (MS) (auxiliary material Figures S1e and S1f) of the total Mg^{2+}. Associated with the crustal Mg^{2+} is Ca^{2+}, which is potentially derived from calcite/gypsum/limestone/dolomite. A much larger portion of NSS contribution in Ca^{2+} than in Mg^{2+} has been observed (auxiliary material Figures S1g and S1h). On average, 63.9 ± 17.0% (NA-1), 51.6 ± 20.0% (P), 88.4 ± 7.2% (SA), 90.3 ± 3.3% (NA-2) and 90.0 ± 8.7% (MS) are NSS portions. Assuming that $NSS\text{-}Mg^{2+}$ and $NSS\text{-}Ca^{2+}$ are of crustal origin, these

[1] Auxiliary materials are available in the HTML. doi:10.1029/2010JD014246.

Table 1. Average, Standard Deviation (SD), Minimum (Min), and Maximum (Max) Atmospheric Ion Species, OC, and EC Concentrations in TSP Samples During Two Cruises[a]

	Cruise I						Cruise II								
	Northern Atlantic (NA-1)			Pacific(P)			Southern Atlantic (SA)			Northern Atlantic (NA-2)			Mediterranean Sea (MS)		
Species	Average ± SD	Min	Max	Average ± SD	Min	Max	Average ± SD	Min	Max	Average ± SD	Min	Max	Average ± SD	Min	Max
TSP, $\mu g\ m^{-3}$	20.1 ± 9.0	11.4	39.8	36.7 ± 18.1	10.4	81.9	39.1 ± 13.5	11.7	57.5	81.9 ± 20.3	48.6	116.1	46.9 ± 28.7	12.7	95.3
total ions, $\mu g\ m^{-3}$	10.5 ± 6.2	5.5	23.4	19.7 ± 12.4	1.5	48.5	16.0 ± 8.9	6.5	34.7	25.9 ± 6.6	12.1	33.1	13.6 ± 9.3	3.9	28.8
Na^+, $\mu g\ m^{-3}$	2.99 ± 1.90	1.20	7.22	5.81 ± 3.97	0.36	15.25	4.50 ± 2.42	1.79	9.11	6.99 ± 1.75	3.59	9.66	4.07 ± 3.00	1.68	10.02
K^+	98.4 ± 74.3	34.1	256.9	231.1 ± 149.0	19.2	597.6	204.9 ± 231.3	15.5	833.8	302.2 ± 103.5	198.1	502.9	129.3 ± 102.3	17.4	288.7
NSS-K^+	−12.4 ± 14.5	−29.5	16.6	16.3 ± 26.6	−10.8	106.5	38.3 ± 239.9	−86.2	727.5	43.7 ± 72.2	−69.4	145.5	−21.3 ± 80.0	−162.9	198.5
Mg^{2+}	435.1 ± 240.7	197.7	971.9	740.3 ± 481.0	52.1	1872.6	783.9 ± 312.2	387.2	1354.6	970.1 ± 213.7	522.8	1229.6	490.1 ± 296.8	230.5	1021.3
NSS-Mg^{2+}	78.8 ± 16.8	55.3	112.9	49.3 ± 45.8	−2.6	239.3	248.3 ± 73.8	164.2	399.0	138.7 ± 71.0	16.1	248.1	5.8 ± 121.3	−171.5	199.4
Ca^{2+}	370.8 ± 115.9	221.2	542.5	441.6 ± 215.4	83.5	1038.0	1532.9 ± 312.7	926.0	1977.1	2699.4 ± 695.2	1500.8	3435.6	1673.3 ± 626.6	1017.1	3317.9
NSS-Ca^{2+}	256.4 ± 92.2	132.0	395.5	219.7 ± 156.6	48.4	858.2	1360.9 ± 314	675.0	1837.5	2432.4 ± 671.4	1363.5	3149.7	1517.8 ± 606.1	660.6	3057.7
NH_4^+	0 ± 0	0.0	0.0	0 ± 0	0.0	0.0	7.6 ± 13.9	0.0	36.2	0.0 ± 0.0	0.0	0	13.7 ± 51.3	0.0	192.1
SO_4^{2-}, $\mu g\ m^{-3}$	1.33 ± 0.75	0.26	2.50	2.10 ± 1.05	0.27	4.54	1.95 ± 1.05	0.68	3.92	3.65 ± 0.76	2.14	4.59	2.02 ± 1.89	0.12	6.86
NSS-SO_4^{2-}, $\mu g\ m^{-3}$	0.57 ± 0.50	−0.39	1.41	0.64 ± 0.48	−0.02	1.84	0.82 ± 0.53	0.07	1.94	1.90 ± 0.48	1.23	2.69	0.99 ± 1.51	−0.42	5.02
NO_3^-,$\mu g\ m^{-3}$	0.66 ± 0.44	0.19	1.65	0.12 ± 0.15	0.00	0.53	1.05 ± 0.72	0.00	2.44	1.45 ± 0.87	0.00	3.18	0.91 ± 0.86	0.02	2.54
NO_2^-	214.6 ± 191.1	5.4	516.2	195.4 ± 264.6	0.0	1328.2	509.8 ± 727.5	0.0	2366.4	372.9 ± 444.0	0.0	1066.5	241.2 ± 293.3	0.0	917.2
Cl^-,$\mu g\ m^{-3}$	3.73 ± 2.97	0.77	10.09	9.04 ± 6.85	0.39	25.52	4.85 ± 3.97	0.93	13.42	8.60 ± 3.33	2.80	14.02	3.48 ± 3.95	0.09	12.82
NSS-Cl^-, $\mu g\ m^{-3}$	−1.64 ± 1.13	−3.86	−0.83	−1.38 ± 0.65	−3.15	−0.14	−3.23 ± 1.05	−4.83	−0.66	−3.93 ± 1.10	−6.10	−2.74	−3.82 ± 2.10	−8.95	−1.83
F^-	16.8 ± 9.1	4.3	29.5	27.9 ± 25.2	2.1	95.1	133.1 ± 109.6	10.6	412.5	122.4 ± 116.0	34.1	416.4	99.0 ± 114.5	13.8	401.1
NSS-F^-	16.4 ± 9.2	4.0	29.0	27.2 ± 25.2	1.2	94.8	132.6 ± 109.5	9.8	412.0	121.5 ± 115.8	33.3	415.2	98.5 ± 114.4	13.5	400.8
Acetate	251.0 ± 215.2	0.0	587.5	341.1 ± 1411.3	0.0	7087.5	9.3 ± 30.7	0.0	101.8	26.0 ± 61.2	0.0	182.7	306.8 ± 947.0	0.0	3564.7
Formate	42.7 ± 67.6	0.0	161.7	2.5 ± 7.1	0.0	26.6	8.2 ± 21.0	0.0	68.4	0 ± 0	0	0	0 ± 0	0.0	0.0
MSA	358.3 ± 204.7	0.0	572.4	583.3 ± 601.7	134.3	2602.0	212.1 ± 301.0	0.0	854.8	272.3 ± 550.6	0.0	1697.5	164.4 ± 587.8	0.0	2204.7
Oxalate	41.3 ± 69.6	0.0	206.9	99.9 ± 102.9	0.0	328.8	198.7 ± 136.7	0.0	490.9	458.6 ± 805.5	0.0	2578.9	41.7 ± 70.4	0.0	182.7
EC	273.3 ± 238.2	47.1	884.6	224.0 ± 189.0	0.0	875.2	70.6 ± 148.2	0.0	401.4	475.0 ± 716.0	0.0	2225.4	1185.2 ± 1593.4	0.0	4915.0
OC, $\mu g\ m^{-3}$	0.93 ± 0.71	0.37	2.87	0.82 ± 0.75	0.05	3.95	2.26 ± 2.06	0.92	7.83	4.58 ± 4.02	1.35	14.16	3.52 ± 4.20	0.19	15.43

[a]Concentrations are in $ng\ m^{-3}$ unless otherwise noted.

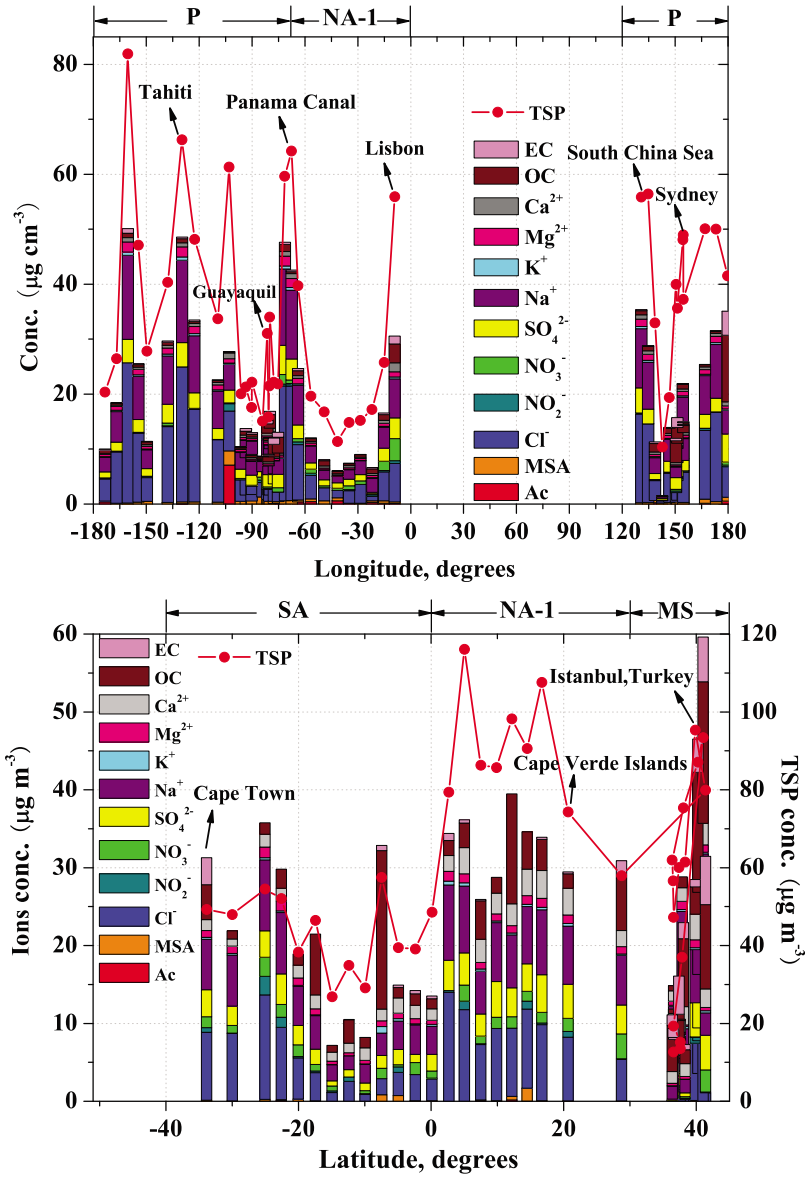

Figure 2. TSP, EC, OC, and total water-soluble ions during (top) cruise I and (bottom) cruise II.

results suggest significant impact of crustal sources, possibly dust from Saharan desert.

3.2.2. Organic and Elemental Carbon

[25] Organic carbon proportions OC1, OC2, OC3 and OC4 were measured by carbon analysis (section 2.3.2). OC1 consists of both aerosols and adsorbed gaseous organics, whereas the rest of the OC (OC2–4) is assumed to be the aerosol phase [*Kirchstetter et al.*, 2001; *Putaud et al.*, 2000]. In order to estimate the particulate organic mass (POM), the OC concentrations obtained from the OC/EC analyzer must be multiplied by an OC-to-POM conversion factor to account for O and H. Different values from 1.2 to 2.1 have been used [*Turpin and Lim*, 2001; *Cavalli et al.*, 2004; *Russell*, 2003; *Virkkula et al.*, 2006]. In this work, the factor 2.1 [*Turpin and Lim*, 2001] was adopted to convert from OC1, OC2, OC3, OC4 and OC2–4 to POM1, POM2, POM3, POM4 and POM2–4, respectively.

[26] Figure 4 shows POM and EC fractions of the total carbon mass (TC) as well as their concentrations during cruise I (Figures 4a and 4c) and cruise II (Figures 4b and 4d). (POM2–4)/TC was normally above 60%, whereas EC/OC was lower than 40%. There was a clear north-south gradient in organic carbon concentrations during cruise II. Organic carbon concentrations in this work are compared with results from two previous measurement campaigns. During a joint U.S./U.S.S.R research cruise in the 1980s, *Rau and Khalil* [1993] observed OC and EC concentration ranges over the North Pacific were 0.5–2.5 μg m^{-3} and 0–0.3 μg m^{-3}, respectively; over the South Pacific, they were <0.6 and <0.02 μg m^{-3}, respectively. In comparison, the OC and EC over the South Pacific in this work ranged of 0.1–3.9 μg m^{-3} and <0.9 μg m^{-3}. In addition, we observed larger EC fractions of TC in the South Pacific. The other campaign was the OC/EC data collected during a cruise over the Atlantic

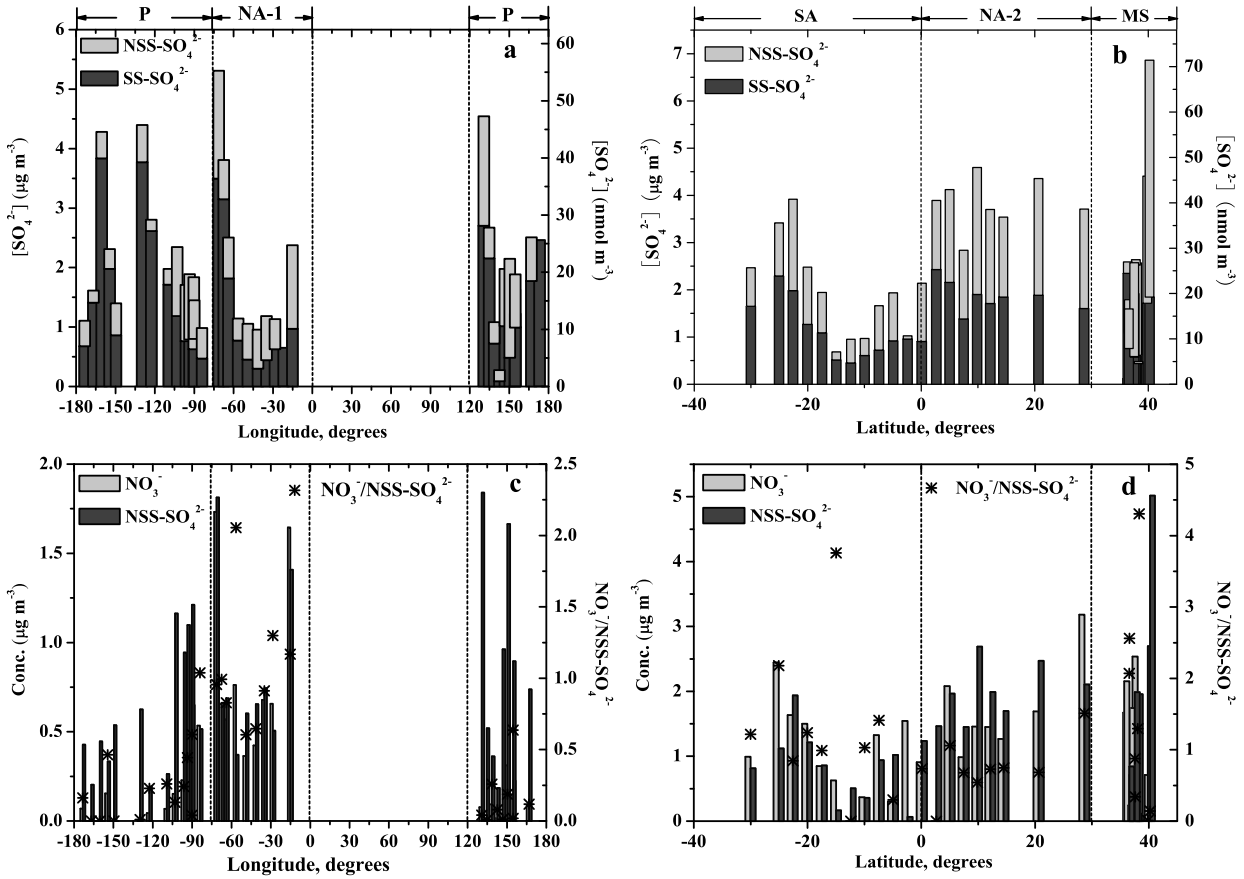

Figure 3. (a, b) SS- and NSS-SO_4^{2-} and (c, d) NO_3^-, NSS-SO_4^{2-}, as well as NO_3^-/NSS-SO_4^{2-} ratios versus longitude for cruise I (Figures 3a and 3c) and latitude for cruise II (Figures 3b and 3d). Five regions are separated by dashed lines.

Table 2. Varimax Rotated Principal Component (Comp) Matrix for Cruise I[a]

	Northern Atlantic Ocean: Cruise I (NA-1)				Pacific Ocean: Cruise I (P)			
	Comp 1 Sea Salt	Comp 2 Anthropogenic	Comp 3 OC and EC	Comp 4 Crustal	Comp 1 Sea Salt	Comp 2 Crustal	Comp 3 F^-	Comp 4 Biomass Burning
Percent of variance	41.9	18.0	13.2	13.0	32.0	19.7	11.2	9.2
Na^+	**(0.947)**	0.220	0.144	−0.147	**(0.980)**	−0.138	0.012	−0.074
K^+	**(0.941)**	0.247	0.154	−0.099	**(0.969)**	−0.128	0.061	0.076
NSS-K^+	**(0.725)**	0.410	0.208	0.291	0.020	0.040	0.274	**(0.835)**
Mg^{2+}	**(0.946)**	0.215	0.149	−0.148	**(0.985)**	−0.055	0.018	−0.059
NSS-Mg^{2+}	**(0.925)**	0.150	0.223	−0.167	0.246	**(0.839)**	0.057	0.142
Ca^{2+}	**(0.868)**	0.235	0.254	0.089	**(0.769)**	**(0.556)**	0.082	0.105
NSS-Ca^{2+}	0.361	0.165	0.352	**(0.489)**	0.110	**(0.898)**	0.101	0.216
SO_4^{2-}	**(0.857)**	**(0.489)**	0.037	−0.063	**(0.890)**	0.007	0.019	0.022
NSS-SO_4^{2-}	0.392	**(0.862)**	−0.189	0.125	−0.094	0.299	0.017	0.200
NO_3^-	0.328	**(0.910)**	−0.007	0.072	−0.337	0.107	0.329	0.026
NO_2^-	**(0.654)**	−0.054	0.409	0.001	−0.152	**(0.935)**	0.141	−0.063
Cl^-	**(0.965)**	0.207	0.032	−0.082	**(0.976)**	−0.133	0.005	−0.095
NSS-Cl^-	−0.363	−0.189	−0.764	0.472	−0.439	0.106	−0.086	−0.196
F^-	−0.186	0.060	−0.269	**(0.936)**	0.021	0.206	**(0.951)**	0.016
NSS-F^-	−0.241	0.045	−0.272	**(0.923)**	0.002	0.208	**(0.950)**	0.017
MSA	**(0.527)**	−0.004	0.225	**(0.569)**	−0.122	**(0.731)**	0.282	−0.255
$C_2O_4^{2-}$	0.170	**(0.913)**	0.256	0.007	0.264	0.248	−0.085	0.100
Cation-anion	0.240	−0.275	**(0.779)**	−0.488	0.350	−0.807	−0.076	0.206
OC	0.060	**(0.629)**	**(0.674)**	−0.063	−0.084	−0.017	−0.274	**(0.856)**
EC	**(0.597)**	0.363	**(0.634)**	0.011	**(0.510)**	−0.172	0.079	**(0.502)**
TSP	**(0.965)**	0.157	0.151	−0.048	**(0.899)**	0.239	−0.074	0.195
Wind speed	**(0.615)**	**(0.557)**	0.364	−0.029	0.386	−0.242	**(0.496)**	−0.093

[a]Rotation converged in nine interactions for NA-1 and eight interactions for P. There are 13 samples for NA-1 and 25 for P. All components (Comp) have eigenvalues >1 and account for a cumulative variance >72.3%. Large values are indicated in bold and parentheses.

Table 3. Varimax Rotated Principal Component Matrix for Cruise II[a]

	Southern Atlantic Ocean (SA)			Northern Atlantic Ocean (NA-2)				Mediterranean Sea (MS)			
	Comp 1 Sea Salt Plus Anthropogenic	Comp 2 Biomass	Comp 3 Crustal	Comp 1 Biomass	Comp 2 Sea Salt Plus SO_4^{2-}	Comp 3 Crustal	Comp 4 Anthropogenic	Comp 1 Sea Salt Plus SO_4^{2-}	Comp 2 Crustal	Comp 3 Anthropogenic	Comp 4 Biomass
Percent of variance	32.6	24.8	17.8	30.3	26.0	17.4	9.5	33.3	21.8	17.0	10.3
Na^+	**(0.971)**	−0.120	−0.036	0.358	**(0.921)**	0.037	0.095	**(0.705)**	−0.566	−0.370	0.009
K^+	0.194	**(0.959)**	0.005	**(0.824)**	0.481	0.111	−0.054	**(0.577)**	−0.525	0.104	**(0.552)**
NSS-K^+	−0.176	**(0.970)**	0.018	**(0.861)**	−0.136	0.126	−0.163	−0.239	0.113	**(0.645)**	**(0.693)**
Mg^{2+}	**(0.978)**	0.073	0.033	0.327	**(0.848)**	0.348	0.147	**(0.658)**	−0.381	−0.575	0.111
NSS-Mg^{2+}	0.340	**(0.779)**	0.282	−0.066	−0.149	**(0.939)**	0.162	−0.464	**(0.732)**	−0.321	0.244
Ca^{2+}	0.151	0.135	**(0.925)**	−0.269	**(0.555)**	**(0.681)**	−0.323	**(0.720)**	**(0.506)**	−0.150	0.426
NSS-Ca^{2+}	−0.136	0.170	**(0.932)**	−0.314	0.483	**(0.702)**	−0.343	**(0.611)**	**(0.630)**	−0.085	0.439
SO_4^{2-}	**(0.943)**	0.041	0.067	−0.221	**(0.920)**	−0.050	0.177	**(0.925)**	−0.117	0.073	−0.054
NSS-SO_4^{2-}	**(0.749)**	0.218	0.173	−0.672	**(0.608)**	−0.111	0.191	**(0.802)**	0.137	0.275	−0.072
NO_3^-	**(0.813)**	0.194	0.011	−0.615	0.071	0.263	**(0.667)**	0.139	−0.564	**(0.691)**	0.296
NO_2^-	**(0.809)**	−0.107	0.216	0.203	0.302	**(0.770)**	−0.103	**(0.669)**	0.242	−0.264	−0.266
Cl^-	**(0.962)**	−0.143	−0.138	0.473	**(0.853)**	0.060	−0.176	**(0.522)**	−0.663	−0.331	0.149
NSS-Cl^-	−0.387	−0.041	−0.373	0.413	−0.047	0.077	−0.808	−0.825	0.203	0.325	0.256
F^-	0.049	−0.095	0.209	**(0.897)**	0.356	−0.229	−0.036	**(0.643)**	0.156	**(0.665)**	−0.007
NSS-F^-	0.047	−0.095	0.209	**(0.897)**	0.354	−0.230	−0.036	0.641	0.158	**(0.666)**	−0.007
MSA	0.071	**(0.840)**	0.382	−0.092	0.020	**(0.582)**	−0.350	−0.176	0.420	−0.016	−0.328
$C_2O_4^{2-}$	**(0.508)**	0.026	−0.046	−0.087	0.161	0.251	0.105	−0.242	−0.108	−0.374	−0.028
Cation-anion	−0.512	0.223	0.467	−0.653	0.092	**(0.591)**	0.257	0.322	0.210	−0.788	0.265
OC	−0.143	**(0.914)**	−0.144	−0.387	0.095	0.097	−0.036	**(0.688)**	0.495	0.299	−0.290
EC	−0.238	**(0.828)**	0.169	0.138	−0.098	−0.079	**(0.965)**	0.337	**(0.673)**	0.182	−0.480
TSP	0.407	**(0.576)**	0.446	0.001	**(0.724)**	0.281	−0.411	**(0.526)**	**(0.783)**	−0.148	0.136
Wind speed	**(0.665)**	−0.431	−0.357	−0.212	0.082	−0.091	**(0.884)**	−0.331	**(0.613)**	−0.286	**(0.508)**

[a]Rotation converged in six interactions for SA, 13 for NA-2, and six for MS. There are 11 samples for SA, 11 for NA-2, and 14 for MS. All components (Comp) have eigenvalues >1 and account for a cumulative variance >75.2%. Large values are indicated in bold and parentheses.

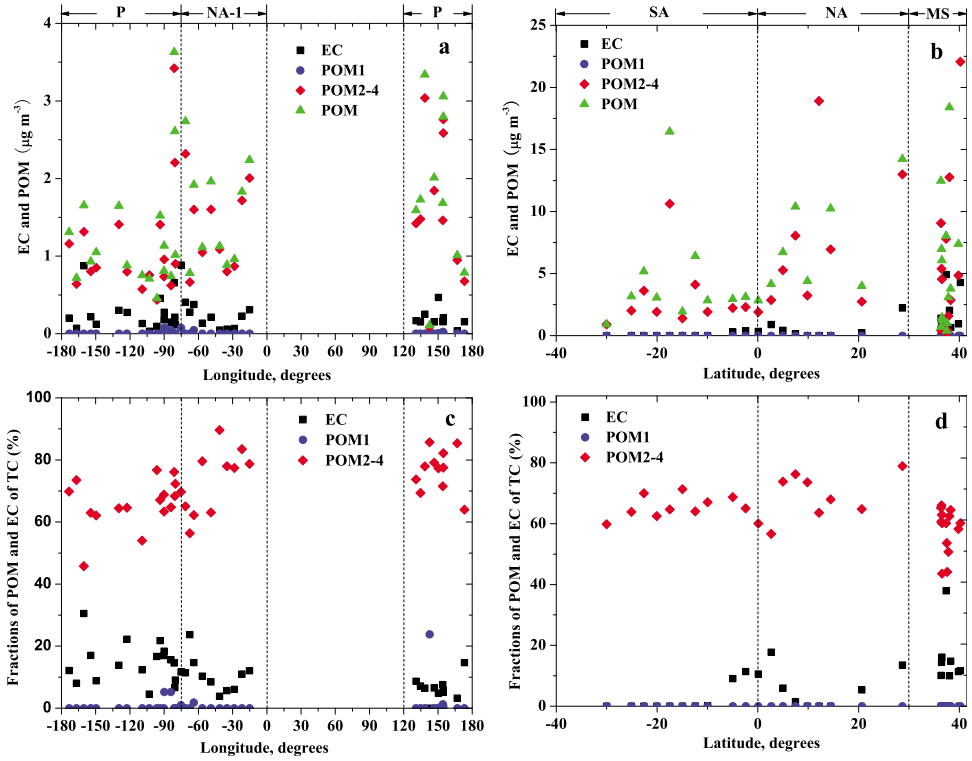

Figure 4. Elemental carbon (EC) and particulate organic carbon (POM) concentrations and their fractions of the total carbon mass during (a, c) cruise I and (b, d) cruise II. POM concentrations were calculated by multiplying the OC concentrations by the factor of 2.1, with POM1, POM2–4, POM as the POMs corresponding to 2.1 × OC1, 2.1 × OC2–4, and 2.1 × OC, respectively. TC is equal to 2.1 × (OC1–4 + OP).

Ocean with a track similar to our cruise II [*Virkkula et al.*, 2006]. They used 1.4 as the organic aerosol mass conversion factor and the major contributor to TC was POM1 (contributing 50% of TC). In contrast, POM2–4 was the main contributor to TC (contributing 60% of TC) in our study. In region 3 (SA), the average POM2–4 concentration was 3.1 ± 2.7 $\mu g\ m^{-3}$, which is much higher than the 123 ± 64 ng m^{-3} reported by *Virkkula et al.* [2006].

3.3. Chloride Deficit

[27] Sea salt aerosol is the major source of halogen radicals [e.g., *Finlayson-Pitts*, 2003] by releasing HCl via reactions between NaCl and sulfuric acid and nitric acid.

$$2NaCl(s) + H_2SO_4 \rightarrow Na_2SO_4 + 2HCl(g) \quad (1)$$

$$NaCl(s) + HNO_3(g) \rightarrow NaNO_3(s) + HCl(g). \quad (2)$$

These reactions result in a deficit of Cl^- relative to the Na^+ compared to the ratio from fresh sea salt aerosols. The Cl^- concentrations in all the samples collected in this study were below the values expected from the sea salt. To examine Cl^- depletion over the different oceans, the percentage of chloride deficit (Cl^- *deficit*%), which is defined as the percentage of the ratio of measured Cl^- concentration in TSP and to the Cl^- expected from sea water [*Millero and Sohn*, 1992] is plotted for five regions in Figure 5 (left). In cruise I, the deficit was 33.5 ± 22.8% (NA-1) and 19.0 ± 11.8% (P), while in cruise II the corresponding values were 37.6 ± 18.0% (SA), 46.0 ± 19.8% (NA-2) and 62.1 ± 20.9% (MS). On some occasions we measured losses of particulate Cl^- approaching 100% in region MS, indicating the influence from air masses heavily polluted by anthropogenic emissions.

[28] The acid displacement reactions are further investigated in Figure 5 (right), which shows the net concentration of mineral acids and the difference between total anions and total cations, as a function of Cl^- deficit. The 1:1 line represents data points for which the Cl^- deficit is exactly matched by the concentration of the specific mineral acids. Thus, points to the right of line indicate that there is not enough mineral acid present to account for the Cl^- deficit found in the samples. NSS-SO_4^{2-} was found to contribute more than NO_3^- (which is located near the 1:1 line), especially in regions P and MS. This indicates that H_2SO_4 may be more important than HNO_3 in creating the Cl^- deficit. However, most of the samples do not contain enough NSS-SO_4^{2-} and NO_3^- to account for the Cl^- deficit. The strong positive correlation between the Cl^- deficit and the surplus of cations, especially in region NA-1 during cruise I, suggests that when Cl^- is released in the form of reactive species, the lost anionic charge is not replaced by a measured species of anion.

3.4. Source Attribution

[29] To find out the possible sources in five regions, relationships between anions, cations, OC, EC, TSP and wind speed were analyzed with principle component analysis (PCA). The outputs of the varimax rotated component matrix are shown in Tables 2 and 3. All tabulated components have eigenvalues larger than 1 and collectively account for a cumulative variance >72.3%. The four main sources are identified in five regions from PCA analysis are (1) sea salt and sea spray, (2) crustal, (3) biomass burning, and (4) anthropogenic. These four sources presented different orders in five regions. Sea salt and sea spray contribution, which is characterized by large loading in Na^+, Cl^-, and wind speed, appears to include biomass burning in region NA-1 and anthropogenic signal in region SA. The component score of sea salt for TSP indicate that sea salt is the major contributor to the total mass loadings observed, except for region SA with the biomass burning component being the major contributor. Crustal component exhibits large loadings of NSS-Ca^{2+} and NSS-Mg^{2+}, with a significant score in region P, SA, NA-2 and MS. This is in agreement with previous studies of dust transport over the Pacific Ocean and the influence of Saharan dust in Africa over the Atlantic Ocean [*Johansen et al.*, 2000; *Virkkula et al.*, 2006]. Signals typically found in biomass burning, such as NSS-K^+, oxalate, OC and EC, have been observed in region SA (24.8% of variance) and NA-2 (30.3% of variance). Finally, the anthropogenic component, exhibits values close to 1 for variables NO_3^-, is notably significant in region MS (17.0% of variance) and NA-1(18.0% of variance).

[30] Based on the above results, the chemical components of the total mass were grouped as sea salt and sea spray ($2.57 \times [Na^+]$) (Figure 3a); the secondary inorganic components (SIC) (NH_4NO_3 + $(NH_4)_2SO_4$, calculated as $1.29 \times NO_3^- + 1.38 \times nssSO_4^{2-}$) [*Yin et al.*, 2005] (Figure 3b); crustal or mineral ($CaSO_4 \cdot 2H_2O$, calculated as $4.3 \times Ca^{2+}$) [*Yin et al.*, 2005] (Figure 3c); and particle organic matter and elemental carbon (POM+EC, $2.1 \times (OC + OP) + EC$) (Figure 3d). Here sea salt (NaCl) was calculated by adding to sodium, chloride and the sea salt contributions of magnesium, calcium, potassium and sulfate, as follows:

$$[Sea\ salt] = [Na^+] + [Cl^-] + 0.12[Na^+] + 0.038[Na^+] + 0.038[Na^+] + 0.25[Na^+], \quad (3)$$

with 0.12, 0.038, 0.038, and 0.25 being the mass ratios in seawater of magnesium to sodium, calcium to sodium, as well as potassium to sodium and sulfate to sodium, respectively [*Millero and Sohn*, 1992]. Because that Cl^- deficit was observed in almost all samples (see section 3.2.2), the average Cl^-/Na^+ ratio 1.12 ± 0.42 (sea water: $Cl^-/Na^+ = 1.79$) during the two cruises was used here for calculation. Thus

$$\begin{aligned}[Sea\ salt] &= [Na^+] + 1.12[Na^+] + 0.12[Na^+] + 0.038[Na^+] \\ &\quad + 0.038[Na^+] + 0.25[Na^+] \\ &= 2.57[Na^+] \end{aligned} \quad (4)$$

The chemical reconstruction by separating sea salt, SIC, crustal and POM+EC in the five regions is shown in Figure 6. The following paragraphs examine the sources for each region by considering the four chemical components and the NAAPS model results.

[31] Regions NA-1 and P during cruise I were characterized by very low SIC, crustal and POM+EC concentrations (Figure 6), except that relatively higher crustal component was observed in region P. Back trajectory and PCA analyses, along with the fact that region NA-1 was mostly under the SE winds as the ship sailed from Lisbon to Balboa, indicate possible long-range transport of Sahara dust. However, when the aerosol optical depth and surface concentrations of sulfate, smoke and dust maps from NAAPS aerosol model were

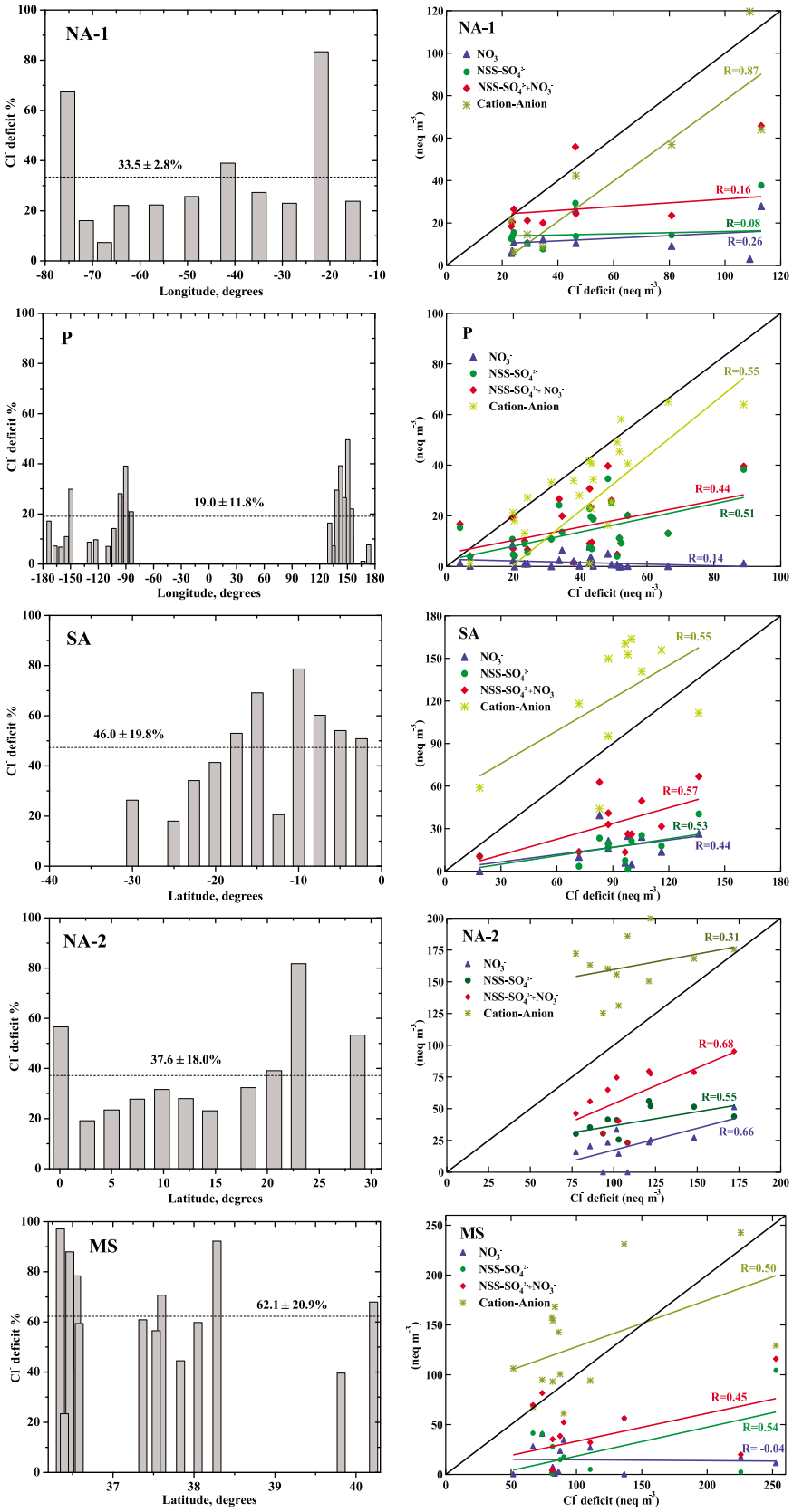

Figure 5. (left) Percent Cl^- deficit versus longitude for cruise I and latitudes for cruise II, with the dashed line for the averaged values. (right) Nanoequivalent (neq) mineral acid concentrations and cation-anion versus Cl^- deficit in five regions. The black line is representative of conditions when mineral acid concentrations equal Cl^- deficit.

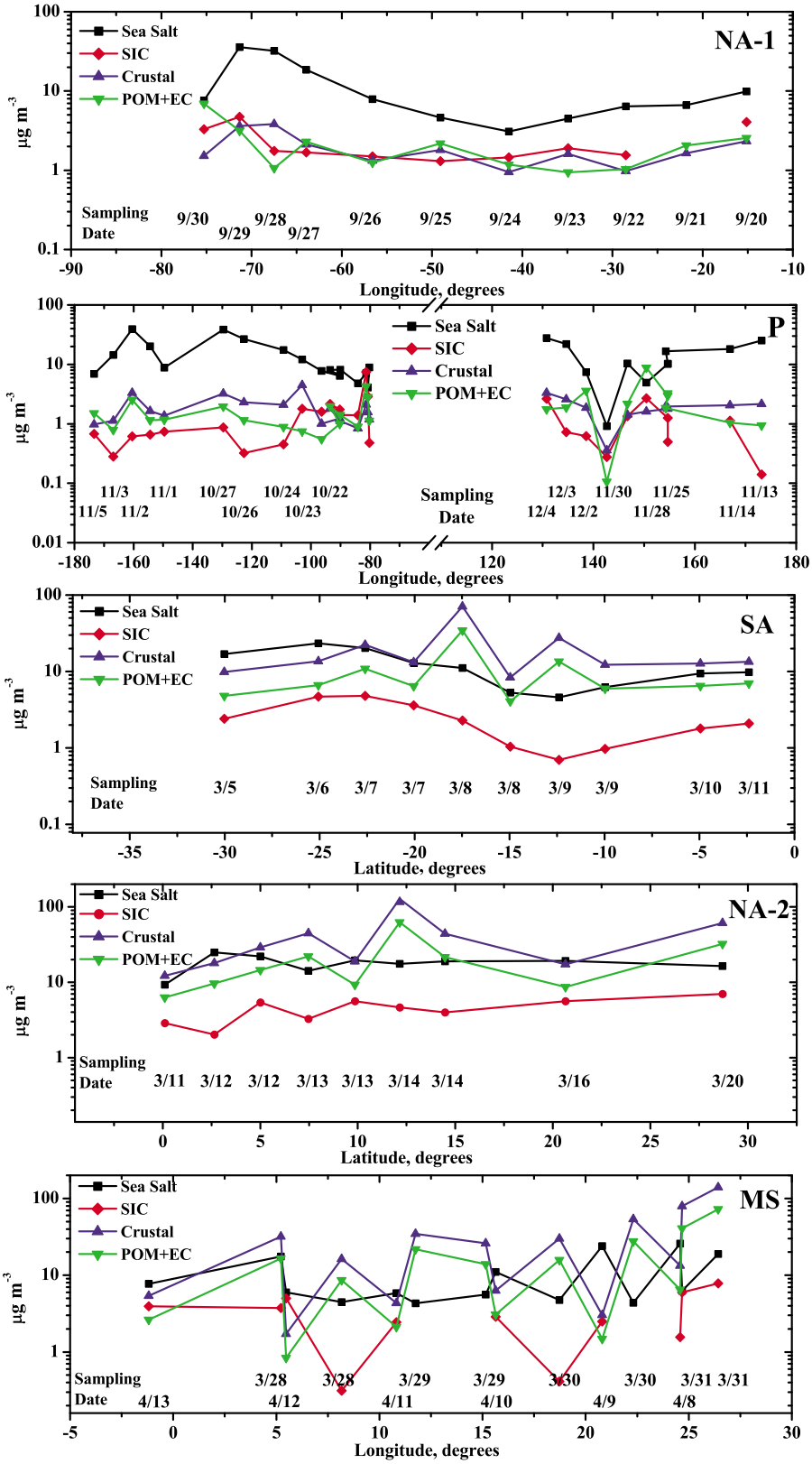

Figure 6. Chemical reconstruction by separating sea salt, secondary inorganic components (SIC), crustal, and particulate organic mass and elemental carbon (POM+EC) in five regions.

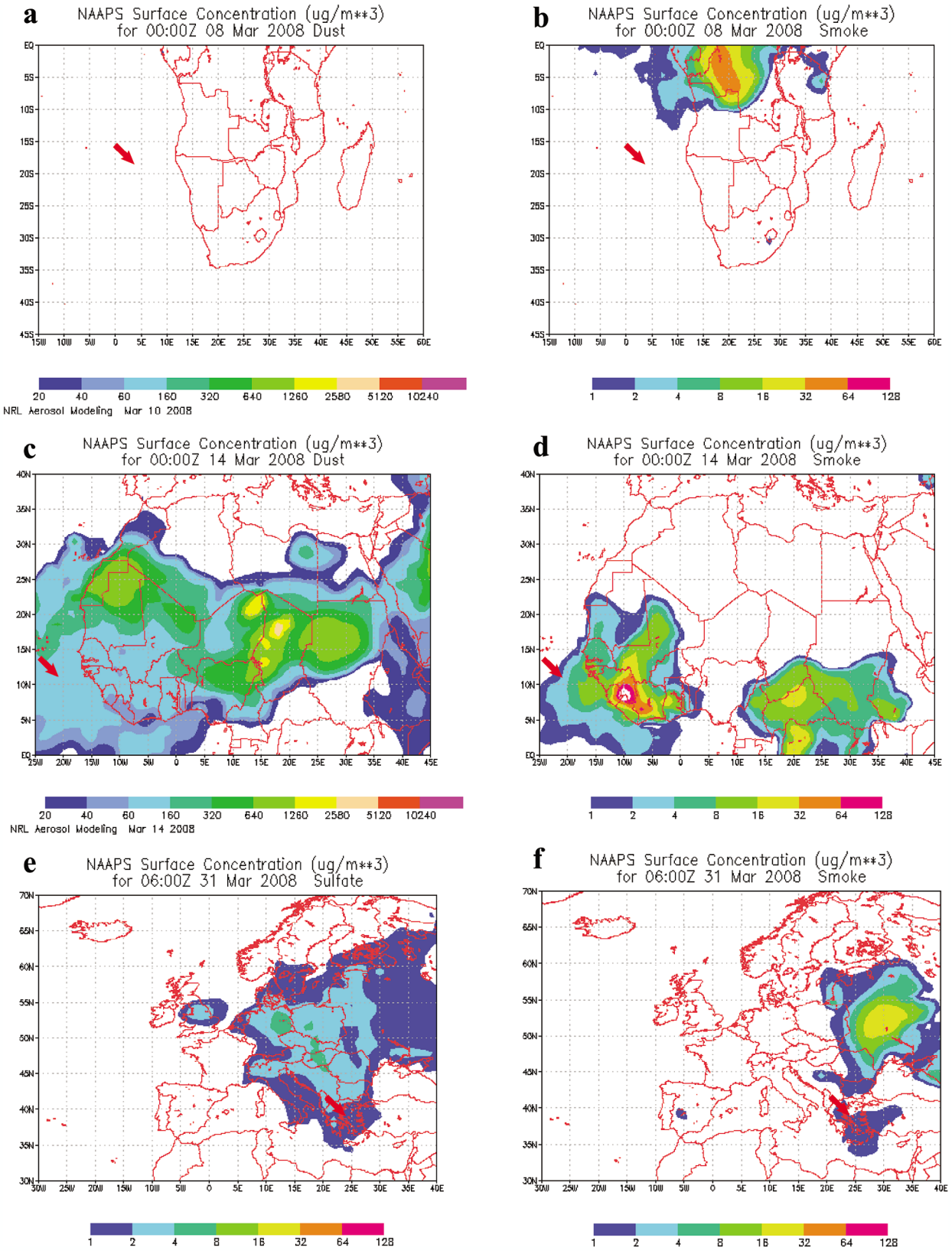

Figure 7. NAAP aerosol optical depth and surface concentration maps: (a) dust and (b) smoke concentrations on 8 March, (c) dust intrusion and (d) smoke concentrations approaching the ship on 14 March, (e) sulfate concentrations from an episode of industrial contamination under stagnant atmospheric conditions, and (f) contamination from biomass burning SW of Moscow. The red arrow represents ship position.

examined in region NA-1 and P, no obvious plumes were observed along the ship track, with dense smoke plumes found mainly in southern rather than central Africa in September 2007 (figures are not shown here). One obvious difference between NA-1 and P is crustal contributions, with the Pacific Ocean affected more by the long-range transport of continental dusts. In conclusion, the cleanest air masses recorded during this cruise campaign were in region NA-1 and P, providing information on oceanic background aerosols. For cruise II, a common feature across regions SA, NA-2 and MS was the strong correlation between POM+EC and crustal materials (Figure 6), suggesting that they are possibly from similar sources. Two cases encountered in these three regions are examined in section 3.2.1.

3.4.1. Cases of Transport of Dust and Biomass Burning

[32] In region SA, when the ship departed from Cape Town, the air masses sampled on the ship were influenced by emissions from southern Africa. As the ship moved closer to the equator, the interhemisphere transport of a dissipating smoke plume originating from biomass burning in central Africa was observed in southern Atlantic region as indicated by enhanced concentrations of K^+ and Oxalate (Figures 7a and 7b and Figure 2). In region NA-2, after a rain event on 11 March near the equator, relatively low concentrations of all components were observed. With the wind direction changing from SW to NE, the ship sampled the mixed Sahara dust and smoke plumes originating from biomass burning in Central Africa on 12–14 March, with the highest TSP level (116.1 μg m^{-3}) observed in NA-2 on 12 March (Figures 7c and 7d and Figure 1). The dust and smoke-laden air masses from central Africa expanded westward into the Atlantic Ocean as the ship sailed along the Africa to NE, thus the relatively higher chemical constituents were observed in region NA-2 (section 3.2).

3.4.2. Cases of Transport of Mixed Industrial and Biomass Burning Pollution

[33] Cruises in the MS region comprised two legs: Barcelona to Istanbul (28–31 March, 2008, Leg 1) and Istanbul to Lisbon (8–13 April, 2008, Leg 2). Much higher POM+EC and crustal concentrations were measured in Leg 1 than in Leg 2. The presence of biomass smoke (Figure 7f) and high concentrations of sulfate (Figure 7e) may explain the rise in the concentrations of crustal material, POM+EC, and SIC. The polluted air masses were of mixed origin/source, with first the smoke originating from biomass burning in the southwest of Moscow, and followed by urban and industrial contamination which spread across much of central and eastern Europe. For Leg 2, although there were contributions from industrial sulfates at beginning, Figure 6 shows a rapid fall in both POM+EC and crustal concentrations on 8 April. When the ship moved toward Lisbon, with the wind direction changed to SW, the ship remained under the influence of Saharan dust, combined with possible smoke plumes, which together may explain the relatively higher crustal and POM+EC on 10–11 April compared with 9 April.

4. Summary and Conclusion

[34] Intensive ship-borne measurements during two cruises in 2007 and 2008 have provided insight into the sources of marine aerosols and the characteristics of air pollution in oceanic areas. The results on TSP mass, ions and elemental and organic carbons have been analyzed with the aid of back trajectory, principle component, and multiple linear regression analyses.

[35] Compared with results from 2 decades ago [*Savoie and Prospero*, 1989; *Prospero and Savoie*, 1989], the NSS-SO_4^{2-} concentrations over the South Pacific appear to have increased by a factor of ~1.5, while NO_3^- remained constant. Assuming that the nitrate values measured in South Pacific (0.12 ± 0.15 μg m^{-3}) are representative of oceanic "background" and that these values are applicable to the oceans in the Northern Hemisphere, the continental sources appear to account for 82% (NA-1), 89% (SA), 91% (NA-2), and 87% (MS) of the total nitrate concentration during the observation periods. A clear north-south gradient was seen in OC concentrations during cruise II. Larger EC fractions of TC were observed in the South Pacific compared with results from 2 decades ago.

[36] The average chloride deficits range from 19.0 ± 11.8% to 62.1 ± 20.9% in five regions. In these samples the deficit can be attributed to acid displacement reactions and discharge between cations and anions. Over the South Pacific and the Mediterranean Sea, NSS-SO_4^{2-} was the preferred species for acid displacement.

[37] During cruise I background values of marine aerosols were only observed over the North Atlantic, while South Pacific was characterized by clean marine air masses and long-range transport signatures. In contrast, results from cruise II suggest that the southern Atlantic Ocean west of the Africa was influenced by the air masses from southern Africa and the interhemispheric transport of smoke plume originating from biomass burning in central Africa. The northern Atlantic Ocean (NA-2) during cruise II experienced combined pollution plumes of Sahara dust and smoke plume originating from biomass burning in central Africa. For the Mediterranean Sea, Leg 1 sampled pollution mixed from biomass burning southwestern of Moscow and the sulfate urban/industrial contamination; whereas Leg 2 measured the influence of Saharan dust and possible smoke plumes.

[38] **Acknowledgments.** This work was supported by the National Natural Science Foundation of China (40875073, 40728006, and 40775080), the Key Science and Technology Project (108050) from the Chinese Ministry of Education, and the International Collaboration Project from the Science and Technology Commission of Shanghai Municipality (09160707700). Data analysis work was partially supported by Hong Kong Polytechnic University's Mainland Joint Supervision Scheme (project GU-635). R. Bhatia, M. Hanvey, and Scholar Ship Program, LLC, were financially supported by Royal Caribbean International. We thank Joseph D. Olander, President of The Scholar Ship, for supporting the onboard research program; Dana Vukajlovich and Stacey Mole for assistance in managing the onboard instruments and for meteorological data collection; Jon Campbell for assistance with the Ferrybox instrumentation; James Canty for marine operations support; and the owner, officers, and crew of The Scholar Ship (*Oceanic II*) for supporting this research through the provision of laboratory infrastructure and operational assistance. We also thank Jay R. Turner from Washington University in St. Louis, Ding Aijun from Nanjing University, and Ravi Kant Pathak and Gao Xiaomei from Hong Kong Polytechnic University for helpful comments.

References

Alonso-Pérez, S., E. Cuevas, X. Querol, M. Viana, and J. C. Guerra (2007), Impact of the Saharan dust outbreaks on the ambient levels of total suspended particles (TSP) in the marine boundary layer (MBL) of the subtropical eastern North Atlantic Ocean, *Atmos. Environ.*, *41*, 9468–9480, doi:10.1016/j.atmosenv.2007.08.049.

Andreae, M. O. (2007), Atmosphere: Aerosols before pollution, *Science*, *315*, 50–51, doi:10.1126/science.1136529.

Arimoto, R., R. A. Duce, D. L. Savoie, J. M. Prospero, R. Talbot, J. D. Cullen, U. Tomza, N. F. Lewis, and B. J. Ray (1996), Relationships among aerosol constituents from Asia and the North Pacific during PEM-West A, *J. Geophys. Res.*, *101*(D1), 2011–2023, doi:10.1029/95JD01071.

Bates, T. S., P. K. Quinn, D. J. Coffman, J. E. Johnson, T. L. Miller, D. S. Covert, A. Wiedensohler, S. Leinert, A. Nowak, and C. Neusüss (2001), Regional physical and chemical properties of the marine boundary layer aerosol across the Atlantic during Aerosols99: An overview, *J. Geophys. Res.*, *106*(D18), 20,767–20,782, doi:10.1029/2000JD900578.

Berresheim, H., M. O. Andreae, R. L. Iverson, and S. M. Li (1991), Seasonal variations of dimethylsulfide emissions and atmospheric sulfur and nitrogen species over the western north Atlantic Ocean, *Tellus, Ser. B*, *43*, 353–372, doi:10.1034/j.1600-0889.1991.t01-3-00002.x.

Cao, J. J., S. C. Lee, K. F. Ho, X. Y. Zhang, S. C. Zou, K. Fung, J. C. Chow, and J. G. Watson (2003), Characteristics of carbonaceous aerosol in Pearl River Delta Region, China, during 2001 winter period, *Atmos. Environ.*, *37*, 1451–1460, doi:10.1016/S1352-2310(02)01002-6.

Cavalli, F., et al. (2004), Advances in characterization of size-resolved organic matter in marine aerosol over the North Atlantic, *J. Geophys. Res.*, *109*, D24215, doi:10.1029/2004JD005137.

Chen, H. H., L. D. Kong, J. M. Chen, R. Y. Zhang, and L. Wang (2007), Heterogeneous uptake of carbonyl sulfide on hematite and hematite—NaCl mixtures, *Environ. Sci. Technol.*, *41*(18), 6484–6490, doi:10.1021/es070717n.

Chiapello, I., and C. Moulin (2002), TOMS and METEOSAT satellite records of the variability of Saharan dust transport over the Atlantic during the last two decades (1979–1997), *Geophys. Res. Lett.*, *29*(8), 1176, doi:10.1029/2001GL013767.

Chiapello, I., C. Moulin, and J. M. Prospero (2005), Understanding the long-term variability of African dust transport across the Atlantic as recorded in both Barbados surface concentrations and large-scale Total Ozone Mapping Spectrometer (TOMS) optical thickness, *J. Geophys. Res.*, *110*, D18S10, doi:10.1029/2004JD005132.

Chow, J. C. (1995), Measurement methods to determine compliance with ambient air quality standards for suspended particles, *J. Air Waste Manage. Assoc.*, *45*, 320–382.

Chow, J. C., J. G. Watson, L.-W. A. Chen, W. P. Arnott, and H. Moosmüller (2004), Equivalence of elemental carbon by thermo/optical reflectance and transmittance with different temperature protocols, *Environ. Sci. Technol.*, *38*(16), 4414–4422, doi:10.1021/es034936u.

Christensen, J. H. (1997), The Danish eulerian hemispheric model—A three-dimensional air pollution model used for the Arctic, *Atmos. Environ.*, *31*, 4169–4191, doi:10.1016/S1352-2310(97)00264-1.

Covert, D. S., V. N. Kapustin, T. S. Bates, and P. K. Quinn (1996), Physical properties of marine boundary layer aerosol particles of the mid-Pacific in relation to sources and meteorological transport, *J. Geophys. Res.*, *101*(D3), 6919–6930, doi:10.1029/95JD03068.

Davison, B., C. N. Hewitt, C. O'Dowd, J. A. Lowe, M. H. Smith, M. Schwikowski, U. Baltensperger, and R. M. Harrison (1996), Dimethyl sulfide, methane sulfonic acid and physicochemical aerosol properties in Atlantic air from the United Kingdom to Halley Bay, *J. Geophys. Res.*, *101*(D17), 22,855–22,867, doi:10.1029/96JD01166.

Duce, R. A., C. K. Unni, B. J. Ray, J. M. Prospero, and J. T. Merrill (1980), Long-range atmospheric transport of soil dust from Asia to the tropical North Pacific: Temporal variability, *Science*, *209*, 1522–1524, doi:10.1126/science.209.4464.1522.

Ebert, M., S. Weinbruch, A. Rausch, G. Gorzawski, G. Helas, P. Hoffmann, and H. Wex (2002), Complex refractive index of aerosols during LACE 98 as derived from the analysis of individual particles, *J. Geophys. Res.*, *107*(D21), 8121, doi:10.1029/2000JD000195.

Ellis, W. G., Jr., R. Arimoto, D. L. Savoie, J. T. Merrill, R. A. Duce, and J. M. Prospero (1993), Aerosol selenium at Bermuda and Barbados, *J. Geophys. Res.*, *98*(D7), 12,673–12,685, doi:10.1029/93JD00951.

Fermo, P., A. Piazzalunga, R. Vecchi, and G. Valli (2006), Set-up of extraction procedures for ions quantification in aerosol samples, *Chem. Eng. Trans.*, *10*, 203–208.

Finlayson-Pitts, B. J. (2003), The tropospheric chemistry of sea salt: A molecular-level view of the chemistry of NaCl and NaBr, *Chem. Rev.*, *103*(12), 4801–4822, doi:10.1021/cr020653t.

Gagosian, R. B., O. C. Zafiriou, E. T. Peltzer, and J. B. Alford (1982), Lipids in aerosols from the tropical North Pacific: Temporal variability, *J. Geophys. Res.*, *87*(C13), 11,133–11,144, doi:10.1029/JC087iC13p11133.

Han, Y. X., X. M. Fang, X. X. Xi, L. C. Song, and S. L. Yang (2006), Dust storm in Asia continent and its bio-environmental effects in the North Pacific: A case study of the strongest dust event in April 2001 in central Asia, *Chin. Sci. Bull.*, *51*, 723–730, doi:10.1007/s11434-006-0723-2.

Hogan, T. F., and T. E. Rosmond (1991), The description of the Navy operational global atmospheric prediction system's spectral forecast model, *Mon. Weather Rev.*, *119*, 1786–1815, doi:10.1175/1520-0493(1991)119<1786:TDOTNO>2.0.CO;2.

Hoornaert, S., H. Van Malderen, and R. Van Grieken (1996), Gypsum and other calcium-rich aerosol particles above the North Sea, *Environ. Sci. Technol.*, *30*(5), 1515–1520, doi:10.1021/es9504350.

Hoornaert, S., R. H. M. Godoi, and R. Van Grieken (2003), Single particle characterization of the aerosol in the marine boundary layer and free troposphere over Tenerife, NE Atlantic, during ACE-2, *J. Atmos. Chem.*, *46*(3), 271–293, doi:10.1023/A:1026383403878.

Huebert, B. J., T. Bates, P. B. Russell, G. Shi, Y. J. Kim, K. Kawamura, G. Carmichael, and T. Nakajima (2003), An overview of ACE-Asia: Strategies for quantifying the relationships between Asian aerosols and their climatic impacts, *J. Geophys. Res.*, *108*(D23), 8633, doi:10.1029/2003JD003550.

Intergovernmental Panel on Climate Change (2007), *IPCC, Climate Change 2007: The Physical Science Basis. Contribution of Working Group I to the Fourth Assessment Report of the Intergovernmental Panel on Climate Change*, edited by S. Solomon et al., 996 pp., Cambridge Univ. Press, Cambridge, U. K.

Jacob, D. J., J. H. Crawford, M. M. Kleb, V. S. Connors, R. J. Bendura, J. L. Raper, G. W. Sachse, J. C. Gille, L. Emmons, and C. L. Heald (2003), Transport and Chemical Evolution over the Pacific (TRACE-P) aircraft mission: Design, execution, and first results, *J. Geophys. Res.*, *108*(D20), 9000, doi:10.1029/2002JD003276.

Jickells, T. D., et al. (2005), Global iron connections between desert dust, ocean biogeochemistry, and climate, *Science*, *308*, 67–71, doi:10.1126/science.1105959.

Johansen, A. M., R. L. Siefert, and M. R. Hoffmann (1999), Chemical characterization of ambient aerosol collected during the southwest monsoon and intermonsoon seasons over the Arabian Sea: Anions and cations, *J. Geophys. Res.*, *104*(D21), 26,325–26,347, doi:10.1029/1999JD900405.

Johansen, A. M., R. L. Siefert, and M. R. Hoffmann (2000), Chemical composition of aerosols collected over the tropical North Atlantic Ocean, *J. Geophys. Res.*, *105*(D12), 15,277–15,312, doi:10.1029/2000JD900024.

Kaneyasu, N., and S. Murayama (2000), High concentrations of black carbon over middle latitudes in the North Pacific Ocean, *J. Geophys. Res.*, *105*(D15), 19,881–19,890, doi:10.1029/2000JD900240.

Kaufman, Y. J., D. Tanré, and O. Boucher (2002), A satellite view of aerosols in the climate system, *Nature*, *419*, 215–223, doi:10.1038/nature01091.

Kirchstetter, T. W., C. E. Corrigan, and T. Novakov (2001), Laboratory and field investigation of the adsorption of gaseous organic compounds onto quartz filters, *Atmos. Environ.*, *35*, 1663–1671, doi:10.1016/S1352-2310(00)00448-9.

Laskin, A., D. J. Gaspar, W. Wang, S. W. Hunt, J. P. Cowin, S. D. Colson, and B. J. Finlayson-Pitts (2003), Reactions at interfaces as a source of sulfate formation in sea-salt particles, *Science*, *301*, 340–344, doi:10.1126/science.1085374.

Lelieveld, J., et al. (2001), The Indian Ocean experiment: Widespread air pollution from south and southeast Asia, *Science*, *291*, 1031–1036, doi:10.1126/science.1057103.

Lerk, C., J. Heinzenberg, and M. Engardt (2002), A meridional profile of the chemical composition of submicrometer particles over the East Atlantic Ocean: Regional and hemispheric variabilities, *Tellus, Ser. B*, *54*, 377–394.

Li, J., J. R. Anderson, and P. R. Buseck (2003), TEM study of aerosol particles from clean and polluted marine boundary layers over the North Atlantic, *J. Geophys. Res.*, *108*(D6), 4189, doi:10.1029/2002JD002106.

Li-Jones, X., and J. M. Prospero (1998), Variations in the size distribution of non-sea-salt sulfate aerosol in the marine boundary layer at Barbados: Impact of African dust, *J. Geophys. Res.*, *103*(D13), 16,073–16,084, doi:10.1029/98JD00883.

Millero, F. J., and M. L. Sohn (1992), *Chemical Oceanography*, CRC Press, Boca Raton, Fla.

Nie, W., T. Wang, X. M. Gao, R. K. Pathak, X. F. Wang, R. Gao, Q. Z. Zhang, and W. X. Wang (2010), Comparison of three filter-based and a continuous technique for measuring atmospheric fine sulfate and nitrate, *Atmos. Environ.*, in press.

Prospero, J. M., and D. L. Savoie (1989), Effects of continental sources on nitrate concentrations over the Pacific Ocean, *Nature*, *339*, 687–689, doi:10.1038/339687a0.

Putaud, J. P., et al. (2000), Chemical mass closure and assessment of the origin of the submicron aerosol in the marine boundary layer and the free troposphere at Tenerife during ACE-2, *Tellus, Ser. B*, *52*, 141–168, doi:10.1034/j.1600-0889.2000.00056.x.

Raes, F., T. Bates, F. McGovern, and M. van Liedckerke (2000), The 2nd aerosol characterization experiment (ACE-2), General overview and main results, *Tellus, Ser. B*, *52*, 111–125.

Rau, J. A., and M. A. K. Khalil (1993), Anthropogenic contributions to the carbonaceous content of aerosols over the Pacific Ocean, *Atmos. Environ., Part A*, *27*(8), 1297–1307.

Riemer, N., O. M. Doherty, and S. Hameed (2006), On the variability of African dust transport across the Atlantic, *Geophys. Res. Lett.*, *33*, L13814, doi:10.1029/2006GL026163.

Russell, L. M. (2003), Aerosol organic-mass-to-organic-carbon ratio measurements, *Environ. Sci. Technol.*, *37*(13), 2982–2987, doi:10.1021/es026123w.

Russell, P. B., P. V. Hobbs, and L. L. Stowe (1999), Aerosol properties and radiative effects in the United States east coast haze plume: An overview of the Tropospheric Aerosol Radiative Forcing Observational Experiment (TARFOX), *J. Geophys. Res.*, *104*(D2), 2213–2222, doi:10.1029/1998JD200028.

Saarikoski, S., M. Sillanpää, M. Sofiev, H. Timonen, K. Saarnio, K. Teinilä, A. Karppinen, J. Kukkonen, and R. Hillamo (2007), Chemical composition of aerosols during a major biomass burning episode over northern Europe in spring 2006: Experimental and modelling assessments, *Atmos. Environ.*, *41*, 3577–3589, doi:10.1016/j.atmosenv.2006.12.053.

Sakai, T., T. Shibata, S.-A. Kwon, Y.-S. Kim, K. Tamura, and Y. Iwasaka (2000), Free tropospheric aerosol backscatter, depolarization ratio, and relative humidity measured with the Raman lidar at Nagoya in 1994–1997: Contributions of aerosols from the Asian Continent and the Pacific Ocean, *Atmos. Environ.*, *34*, 431–442, doi:10.1016/S1352-2310(99)00328-3.

Savoie, D. L., and J. M. Prospero (1989), Comparison of oceanic and continental sources of non-sea-salt sulphate over the Pacific Ocean, *Nature*, *339*, 685–687, doi:10.1038/339685a0.

Sievering, H., J. Boatman, J. Galloway, W. Keene, Y. Kim, and M. Luria (1991), Heterogeneous sulfur conversion in sea-salt aerosol particles: The role of aerosol water content and size distribution, *Atmos. Environ., Part A*, *25*, 1479–1487, doi:10.1016/0960-1686(91)90007-T.

Sievering, H., E. Gorman, T. Ley, A. Pszenny, M. Springer-Young, J. Boatman, Y. Kim, C. Nagamoto, and D. Wellman (1995), Ozone oxidation of sulfur in sea-salt aerosol particles during the Azores Marine Aerosol and Gas Exchange experiment, *J. Geophys. Res.*, *100*(D11), 23,075–23,081, doi:10.1029/95JD01250.

Sievering, H., J. Cainey, M. Harvey, J. McGregor, S. Nichol, and P. Quinn (2004), Aerosol non-sea-salt sulfate in the remote marine boundary layer under clear-sky and normal cloudiness conditions: Ocean-derived biogenic alkalinity enhances sea-salt sulfate production by ozone oxidation, *J. Geophys. Res.*, *109*, D19317, doi:10.1029/2003JD004315.

Smirnov, A., et al. (2006), Ship-based aerosol optical depth measurements in the Atlantic Ocean: Comparison with satellite retrievals and GOCART model, *Geophys. Res. Lett.*, *33*, L14817, doi:10.1029/2006GL026051.

SPSS, Inc. (1997), *SPSS for Windows*, Chicago, Ill.

Talbot, R. W., et al. (1997), Chemical characteristics of continental outflow from Asia to the troposphere over the western Pacific Ocean during February–March 1994: Results from PEM-West B, *J. Geophys. Res.*, *102*(D23), 28,255–28,274, doi:10.1029/96JD02340.

Tsunogai, S., and T. Kondo (1982), Sporadic transport and deposition of continental aerosols to the Pacific Ocean, *J. Geophys. Res.*, *87*(C11), 8870–8874, doi:10.1029/JC087iC11p08870.

Turpin, B. J., and H.-J. Lim (2001), Species contributions to $PM_{2.5}$ mass concentrations: Revisiting common assumptions for estimating organic mass, *Aerosol Sci. Technol.*, *35*, 602–610, doi:10.1080/02786820152051454.

Virkkula, A., K. Teinilä, R. Hillamo, V.-M. Kerminen, S. Saarikoski, M. Aurela, J. Viidanoja, J. Paatero, I. K. Koponen, and M. Kulmala (2006), Chemical composition of boundary layer aerosol over the Atlantic Ocean and at an Antarctic site, *Atmos. Chem. Phys.*, *6*, 3407–3421, doi:10.5194/acp-6-3407-2006.

Yamato, M., and H. Tanaka (1994), Aircraft observations of aerosols in the free marine troposphere over the North Pacific Ocean: Particle chemistry in relation to air mass origin, *J. Geophys. Res.*, *99*(D3), 5353–5377, doi:10.1029/93JD03191.

Yin, J., A. G. Allen, R. M. Harrison, S. G. Jennings, E. Wright, M. Fitzpatrick, T. Barry, D. Ceburnis, and D. McCrusker (2005), Major component composition of urban PM_{10} and $PM_{2.5}$ in Ireland, *Atmos. Res.*, *78*, 149–165, doi:10.1016/j.atmosres.2005.03.006.

Yuan, H., Y. Wang, and G. S. Zhuang (2003), The simultaneous determination of organic acid, MSA with the inorganic anions in aerosol and rainwater by ion chromatography (in Chinese), *J. Instrum. Anal.*, *22*, 11–14.

Zhang, X. Y., G. S. Zhuang, J. H. Guo, K. D. Yin, and P. Zhang (2007), Characterization of aerosol over the northern South China Sea during two cruises in 2003, *Atmos. Environ.*, *41*, 7821–7836, doi:10.1016/j.atmosenv.2007.06.031.

Zhuang, G. S., Z. Yi, R. A. Duce, and P. R. Brown (1992), Link between iron and sulphur cycles suggested by detection of Fe(II) in remote marine aerosols, *Nature*, *355*, 537–539, doi:10.1038/355537a0.

R. S. Bhatia, National Oceanography Centre, Southampton, SO14 3ZH, UK.

J. M. Chen (corresponding author), T. T. Cheng, L. Lin, and M. Zhang, Department of Environmental Science and Engineering, Fudan University, Shanghai 200433, China. (jmchen@fudan.edu.cn)

M. Hanvey, Nature Publishing Group, London, N1 9XW, UK.

T. Wang, Department of Civil and Structural Engineering, Hong Kong Polytechnic University, Kowloon, Hong Kong.